Supplementary information

Searching for genetic evidence of demographic decline in an arctic seabird: beware of overlapping generations

Emeline Charbonnel[1,4], Claire Daguin[2], Lucille Caradec[2], Eléonore Moittié[2], Olivier Gilg[3,4], Maria V. Gavrilo[5], Hallvard Strøm[6], Mark L. Mallory[7], R. I. Guy Morrison[8], H. Grant Gilchrist[8,9], Raphael Leblois[10], Camille Roux[11], Jonathan M. Yearsley[12], Glenn Yannic[1,4a*], Thomas Broquet[2a]

[1] Univ. Grenoble Alpes, Univ. Savoie Mont Blanc, CNRS, LECA, 38000 Grenoble, France

[2] CNRS, Sorbonne Université, UMR 7144, Station Biologique de Roscoff, Place Georges Teissier, 29680 Roscoff, France

[3] Laboratoire Biogéosciences, UMR CNRS 6282, Equipe Ecologie Evolutive, Université de Bourgogne, Boulevard Gabriel, 21000 Dijon, France

[4] Groupe de Recherche en Ecologie Arctique (GREA), 21440 Francheville, France

[5] Arctic and Antarctic Research Institute (AARI), 198397 Saint-Petersburg, Russia

[6] Norwegian Polar Institute, Fram Centre, 9296 Tromsø, Norway

[7] Department of Biology, Acadia University, 33 Westwood Avenue, Wolfville, Nova Scotia B4P 2R6, Canada

[8] Environment Canada, National Wildlife Research Centre, Ottawa, Ontario, K1A0H3, Canada

[9] Department of Biology, Carleton University, Ottawa, Ontario, K1S5B6, Canada

[10] CBGP, INRAE, CIRAD, IRD, Institut Agro, Montpellier SupAgro, Univ. Montpellier, Montferrier-sur-Lez Cedex, France

[11] Univ. Lille, CNRS, UMR 8198 - Evo-Eco-Paleo, F-59000 Lille, France

[12] School of Biology and Environmental Science, University College Dublin, Belfield, Dublin, Ireland

[a] shared senior authorship

* Corresponding author: Glenn Yannic, glenn.yannic@univ-smb.fr

ddRADSeq library construction and sequencing

We constructed two double-digest RAD sequencing (Restriction site Associated DNA; ddRADSeq) libraries from ivory gull genomic DNA following the general protocol from Peterson et al. (2012) and modified in Brelsford et al. (2016). Briefly, individual genomic DNA (50-100 ng) from 167 birds (96 adults and 71 juveniles) was digested using enzymes *SbfI* and *MseI*, ligated to barcoded adaptors, and amplified with Illumina indexed primers. Individual PCR products were then equally pooled into two libraries. Fragments of 300 -750 bp were selected using a Pippin Prep system (Sage Science, Beverly, MA, USA).

With this protocol, samples are pooled only after being treated individually from DNA digestion to final PCR amplification. This allows us to minimize the heterogeneity between samples despite the variability of our DNA sources (buccal swabs and blood). To control for genotype quality, we replicated 17 (9.2 %) of our samples following the recommendations of Mastretta-Yanes et al. (2015). We also included six negative controls (3.14%) in the libraries. In the end, the 2 pooled libraries contained 95 and 96 samples each and were sequenced on two lanes of an Illumina Hi-Seq 2500 producing paired-end (2 x 125bp) sequences (Fasteris SA, Switzerland).

ddRADSeq data processing

The quality of raw sequencing data was controlled using *fastqc* (Andrews, 2010) and *multiqc* (Ewels *et al.*, 2016). We then used Stacks v. 2.4 (Catchen *et al.*, 2011, 2013) to demultiplex data and build a de novo SNP catalog. We obtained on average 2.09 millions of pairs of reads per sample excluding negative controls (min: $0.17 \cdot 10^6$, max: $5.52 \cdot 10^6$, and sd: $0.94 \cdot 10^6$). We tested different sets of Stacks core parameters, by varying one parameter at a time (by steps of one unit: ustack − m (2–6), −M (2–6), −max_locus_stacks (2–6), and cstack −n (0–5)),

whereas the others remained at their default values, as suggested by Mastretta-Yanes et al. (2015). Using the default SNP calling model, we identified the optimal values of −m (4), −M (2), −max_locus_stacks (3) and −n (2) as those that minimized genotype differences between replicates (n = 17 pairs) and maximized the amount of data recovered. To produce the final data set, we ran Stacks with all parameters set to their optimal values, and with the minimum allelic frequency set to 0.01 and maximum observed heterozygosity set to 0.8. The next filtering steps were performed in R (R Development Core Team, 2020) from the original VCF file using R package vcfR (Knaus and Grünwald, 2017), and consisted in keeping only loci that were typed for at least 93% of samples according to missing data distribution, and only samples that were typed for at least 90% of loci. This very stringent filtering aimed to produce a high-quality, homogeneous SNP dataset despite the heterogeneity of the DNA sources used.

Detailed settings used in *Migraine* software (Leblois *et al.*, 2014)

WriteSequence=Over,Append,Append,Append

GenepopFileName=data_Migraine

DemographicModel=OnePopVarSize

VarSizeFunction=Discret

MutationalModel=GSM

GivenK=40

StepSizes=4,4,4,4,4,4,4,4,4,4

Statistic=PACanc

PointNumber=2000

NRunsPerPoint=5000

MaxKrigPtNbr=5000

GridSteps=35

Plots=Allprofiles

1DCI=pGSM,2Nmu,Tchange,2Nancmu,Nratio,Tgmu

LowerBound=0.01,11.0,0.001,5.0

UpperBound=0.16,200.0,0.2,40.0

SamplingScale=logscale,logscale,logscale,logscale

graphicFormat=pdf

Detailed settings used in *DILS* software (Fraïsse *et al.*, 2021)

region: noncoding

nspecies: 1

nameA: Peburnea

nameOutgroup: NA

lightMode: FALSE

max_N_tolerated: 0.2

Lmin: 150

nMin: 154

mu: 000001

rho_over_theta: 0.8

N_min: 0

N_max: 100000

Tchanges_min: 0

Tchanges_max: 200000

Simulation of microsatellite data in bottlenecked populations

Stochastic forward-in-time simulations of population demography and genetic markers were performed with a modified version of *Nemo* (Nemo-age, Cotto *et al.*, 2020) that incorporates age structure. We considered a life-cycle where adults reproduce each year with fecundity randomly drawn from a Poisson distribution of mean 2 and then may survive to the next time step (year) with probability *v*. Offspring do not reproduce during their first year of life (age at maturity *a*=1). We considered a single population that may vary in size up to a carrying capacity limit of 1000 individuals (and then 500 or 250 depending on the bottleneck scenario simulated). These simulations are fully stochastic: population size is set by the number of birds that are born and survive, and thus simulated populations may go extinct simply because of demographic stochasticity (especially post-bottleneck). To avoid that, we adjusted offspring survival (i.e. probability of surviving to the adult class) so that the growth rate of the population is constant and equal to λ=1.025. Hence with adult survival v = 0.80 we set offspring survival to v_{juv}*=0.231* and with v = 0.95 we used v_{juv}=0.077. These simulation conditions led to the age structures represented in Figure S3.

In these simulations, generation time differs slightly from the prediction for a strictly constant population size, where $T_G = 1/(1-v)$ if newborns become reproductively mature within one breeding cycle (see introduction in main text). If sexual maturity if delayed to age *a*, then as shown *e.g.* by Nunney (1993), the average adult lifespan is $1/(1-v)$, and $T_G = a - 1 + 1/(1-v)$, equivalent to $T_G = a + \left(\frac{v}{1-v}\right)$. To comply with the conditions of our simulations we use $T_G = a + \left(\frac{v}{\lambda - v}\right)$ (e.g., Gaillard *et al.*, 2005), which gives:

Simulation scenario 1: no adult survival, T_G =1 year.

Simulation scenario 2: v = 0.8, T_G = 4.56 years.

Simulation scenario 3: v = 0.95, T_G = 13.67 years.

The generation time estimated empirically from the simulations (*i.e.* mean age of adults, considering that all adults have the same probability of producing offspring at the next generation) were close to the theoretical predictions:

Simulation scenario 2: T_G = 4.49 years.

Simulation scenario 3: T_G = 13.41 years.

In all cases we ran simulations for several time units large enough so that ΔH reaches mutation-drift equilibrium before imposing a bottleneck to the population. Depending on the scenario, each simulation was run from 10 000 to 135 000-time steps before the bottleneck occurred.

Table S1. Number of alleles (*nA*), number of effective alleles (*nEffA*, *i.e.*, the number of alleles weighted by their frequencies), and Nei's estimations of heterozygosity: observed (H_O), within samples heterozygosity (H_S) and total (H_T) heterozygosity for each marker used in this study across the entire range of ivory gull (based on 15 adults sampling sites).

Locus	*repeat*	*nA*	*nEffA*	H_O	H_S	H_T
A111	di-	9	2.449	0.628	0.626	0.621
B125	tetra-	13	5.142	0.790	0.854	0.858
C7	tetra-	9	3.334	0.797	0.735	0.753
D126	tetra-	13	4.737	0.852	0.831	0.843
D5	tetra-	11	5.231	0.832	0.856	0.866
D9	tetra-	9	3.608	0.732	0.766	0.752
A129	di-	5	2.009	0.428	0.536	0.542
A132	di-	3	2.196	0.581	0.574	0.576
D103	tetra-	23	6.320	0.882	0.903	0.916
D110	tetra-	18	5.269	0.500	0.880	0.884
C6	tetra-	12	4.641	0.761	0.833	0.846
D6	tetra-	14	4.905	0.536	0.858	0.847
A115	di-	15	3.407	0.749	0.745	0.756
B103	tetra-	7	3.355	0.684	0.744	0.754
D1	tetra-	14	4.234	0.749	0.810	0.819
Overall		11.7	4.056	0.700	0.770	0.775

Table S2. Pairwise genetic differentiation (F_{ST}) among populations with n > 10 samples. Lower half-matrix based on microsatellites; upper half-matrix based on SNPs. Significant differentiations are bolded.

		Greenland		Norway		Russia			Canada	
		1_StNo	2_StBr	4_Auga	6_Free	8_Rudo	10_SchI	11_Doma	14_SeyI	15_AlEI
Greenland	1_StNo		0.0029	0.0067	0.0052	-	-	-	-	0.0073
	2_StBr	-0.0014		0.0065	0.0055	-	-	-	-	0.0036
Norway	4_Auga	-0.0008	0.0012		-0.0005	-	-	-	-	0.0057
	6_Free	**0.0042**	0.0026	-0.0033		-	-	-	-	0.0040
Russia	8_Rudo	**0.0078**	0.0008	0.0032	0.0002		-	-	-	-
	10_SchI	**0.0066**	-0.000	0.0002	-0.0026	0.0082		-	-	-
	11_Doma	**0.0050**	0.0052	0.0035	0.0062	0.0078	0.0031		-	-
Canada	14_SeyI	0.0092	0.0072	-0.0016	-0.0025	0.0041	-0.0036	0.0102		-
	15_AlEI	0.0006	0.0032	-0.0007	-0.0031	0.0026	-0.0005	**0.0070**	0.0001	

Table S3. Pairwise genetic differentiation (F_{ST}) among regions. Lower half-matrix based on microsatellites; upper half-matrix based on SNPs. Significant differentiations are bolded.

	Greenland	**Norway**	**Russia**	**Canada**
Greenland		0.0059	-	0.0047
Norway	**0.0036**		-	**0.0058**
Russia	**0.0049**	0.0015		-
Canada	0.0054	0.0004	0.0033	

Table S4. Adjusted *p-values* for multiple comparisons using the Benjamini and Hochberg false discovery rate procedure with initial α = 0.05 on *Bottleneck* analyses results. Same hypothesis was tested several times on different data sets (i.e., at different scales) and using two different mutation models (TPM 70% et TPM 95%). In addition, for the Alert, Ellesmere Island population, we considered a TPM 0% model. Population names refer to the locality names in table 1. We provided original p-values (*p values*) as well as corrected p-values (*fdr-p values*), obtained using the function *p.adjust()* and the "fdr" method in the "stats" R package. * in bold depict significant *p-values.*

Scale	Population	Mutation model	*p values*	*fdr-p values*
Global	Whole	TPM70	0.036*	0.132
	Whole	TPM95	0.932	0.966
Regional	Greenland	TPM70	**0.011***	0.062
	Norway		0.084	0.245
	Russia		0.281	0.452
	Canada		0.126	0.305
	Greenland	TPM95	0.972	0.972
	Norway		0.598	0.826
	Russia		0.906	0.966
	Canada		0.489	0.709
Population	1_StNo	TPM70	0.011*	0.062
	2_StBr		**0.004***	0.059
	4_Auga		0.104	0.274
	6_Free		0.211	0.407
	8_Rudo		**0.028***	0.132
	10_SchI		0.180	0.401
	11_Doma		0.211	0.407
	14_SeyI		0.084	0.245
	1_StNo	TPM95	0.924	0.966
	2_StBr		0.661	0.833
	4_Auga		0.756	0.897
	6_Free		0.773	0.897
	8_Rudo		0.281	0.452

10_SchI		0.489	0.709
11_Doma		0.661	0.833
14_SeyI		0.281	0.452
15_AlEI	TPM00	**0.006***	0.059
15_AlEI	TPM70	**0.001***	**0.024***
15_AlEI	TPM95	**0.032***	0.132

Table S5. One-tailed p-values obtained when testing an excess of heterozygotes with a Wilcoxon test in *Bottleneck*, based on genetic data obtained from stochastic simulations of microsatellite markers evolving under IAM or SMM in a single population that went from 1000 to 250 individuals or from 1000 to 500 individuals at the peak of ΔH and 20 years after the decline, under three survival models, where *v* correspond to adult survival *v*=0.8 and *v*=0.95 in overlapping generation models.

Mutation model	Bottleneck strength	Time after bottleneck	Adult survival	One-tailed p-values< 0.05 (x / 10)
IAM	1000->250	+ 20 years	no overlapping	8
			overlapping (*v* =0.8)	3
			overlapping (*v* =0.95)	1
		peak ΔH	no overlapping	9
			overlapping (*v* =0.8)	8
			overlapping (*v* =0.95)	7
	1000->500	+ 20 years	no overlapping	3
			overlapping (*v* =0.8)	3
			overlapping (*v* =0.95)	0
		peakΔH	no overlapping	4
			overlapping (*v* =0.8)	0
			overlapping (*v* =0.95)	4
SMM	1000->250	+ 20 years	no overlapping	1
			overlapping (*v* =0.8)	1
			overlapping (*v* =0.95)	0
		peakΔH	no overlapping	2
			overlapping (*v* =0.8)	2
			overlapping (*v* =0.95)	0
	1000->500	+ 20 years	no overlapping	0
			overlapping (*v* =0.8)	0
			overlapping (*v* =0.95)	0
		peakΔH	no overlapping	0
			overlapping (*v* =0.8)	0
			overlapping (*v* =0.95)	1

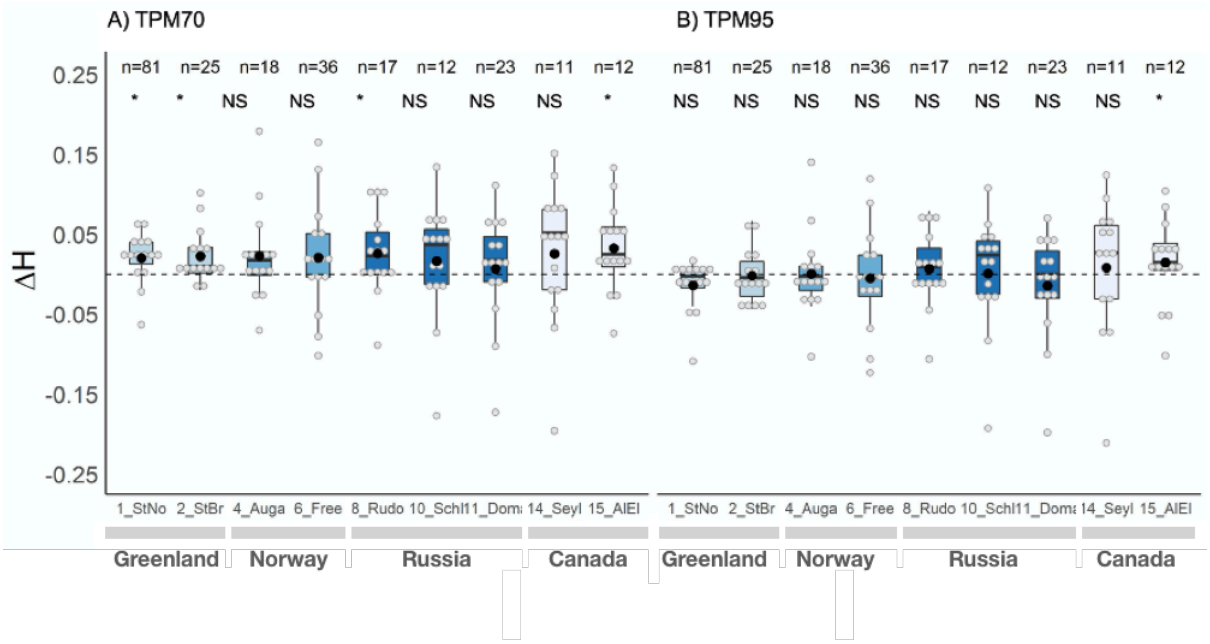

Figure S1. Heterozygosity-excess (ΔH) at 15 microsatellite loci in nine populations of ivory gull, obtained with *Bottleneck* software for two mutational models (A) TPM70 and (B) TPM95. The average Δ*H* over all loci is represented by a black dot, and locus-specific values are represented by smaller grey dots. The dashed line represents equality between observed and expected heterozygosity, i.e. $\Delta H = H_E - H_{Eq} = 0$. Symbols (*) and (NS) indicate that the one tail probability of $H_E > H_{Eq}$, *i.e.* heterozygosity-excess, is significant (*p*-value < 0.05) or not significant, using Wilcoxon's test.

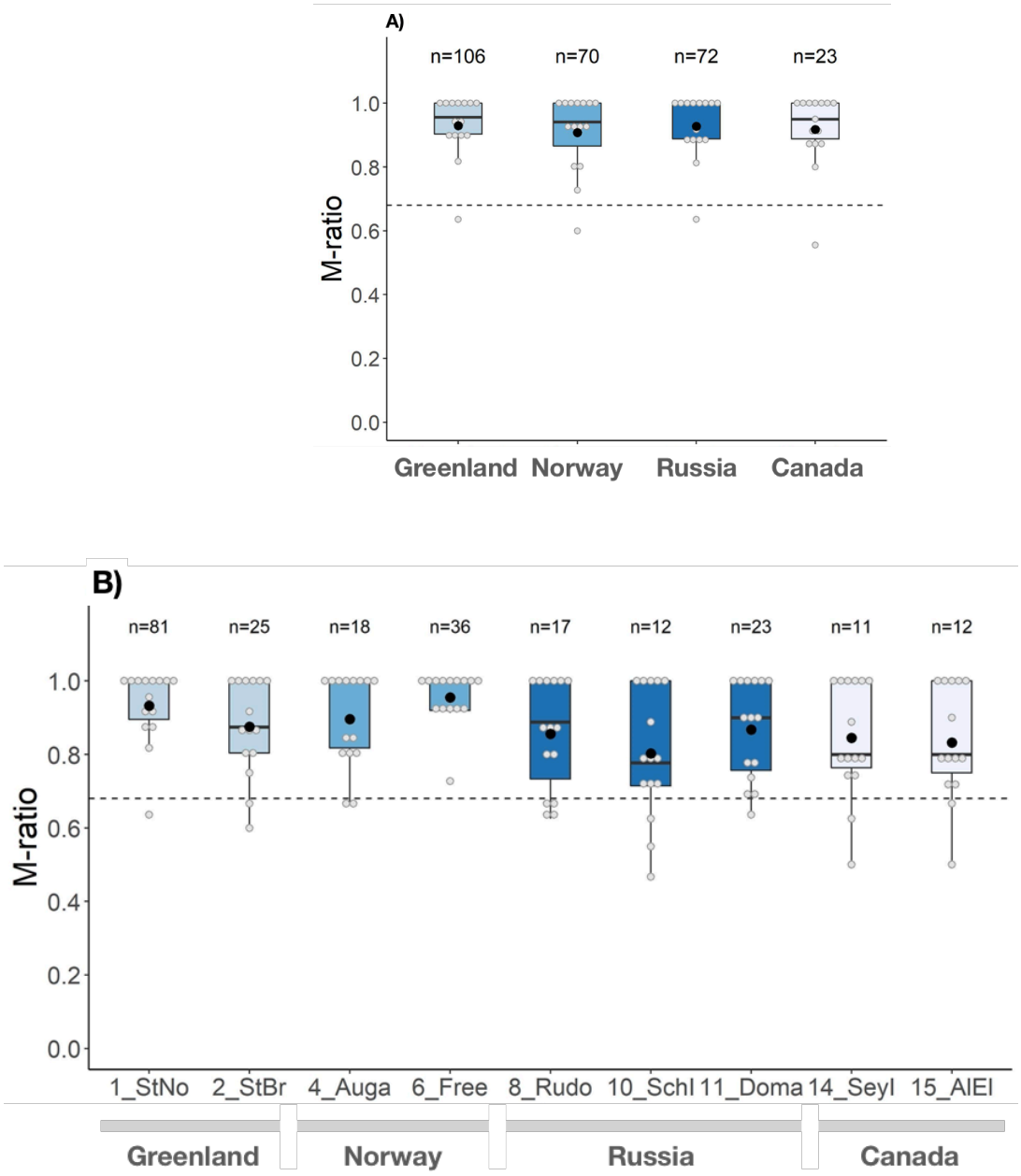

Figure S2. Average Garza and Williamson's *M*-ratio calculated using 15 microsatellite loci, for A) breeding regions and B) populations with a large enough number of samples (*n*> 10). The average *M*-ratio over all loci is shown in black, while locus-specific values are represented by smaller grey dots. The dashed line represents *M*-ratio critical value (*M* = 0.68; Garza & Williamson 2001); under this value, it can be supposed that a population has experienced a recent demographic decline.

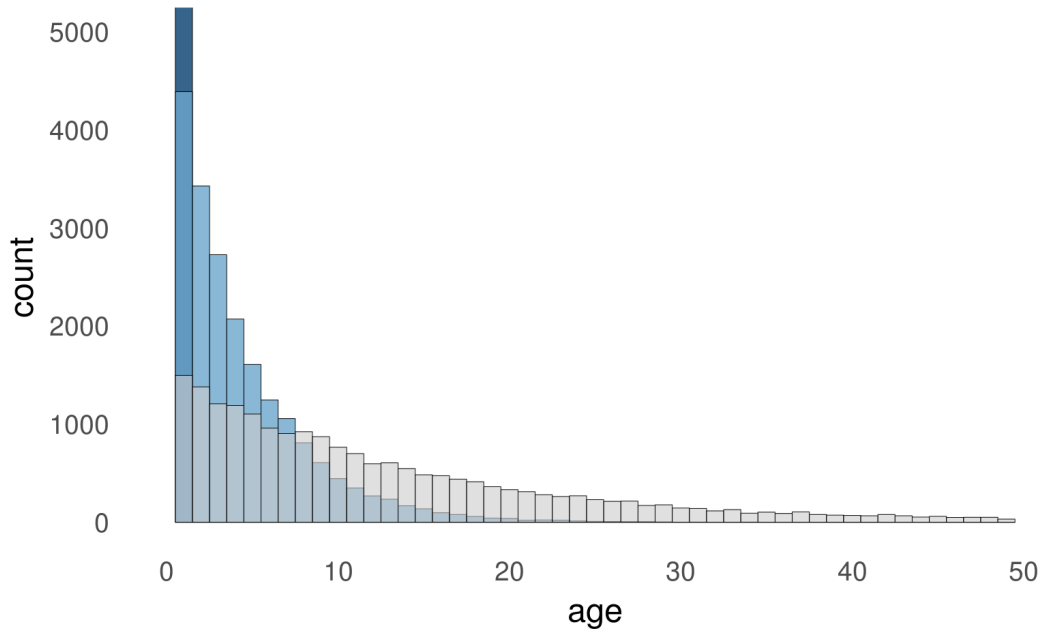

Figure S3. Distribution of the age of reproducing adults when v = 0 (no age structure, in dark blue), v = 0.8 (light blue), and v = 0.95 (grey). These distributions were obtained from the stochastic simulations produced by *Nemo-age* (Cotto *et al.*, 2020) to study the dynamics of ΔH (see main text). Here we used 10 replicates of 1000 adults (before bottleneck) from 2 simulations scenarios (hence 20000 individuals for each survival value). Note that with v = 0 all adults in the population are one year old (i.e. the dark blue bar goes up to 20000), and with v = 0.95 there are some rare individuals that grow much older than 50 years old (not represented here for the sake of readability). The light blue histogram (v = 0.8) approximately imitates the ivory gull situation, assuming constant adult survival.

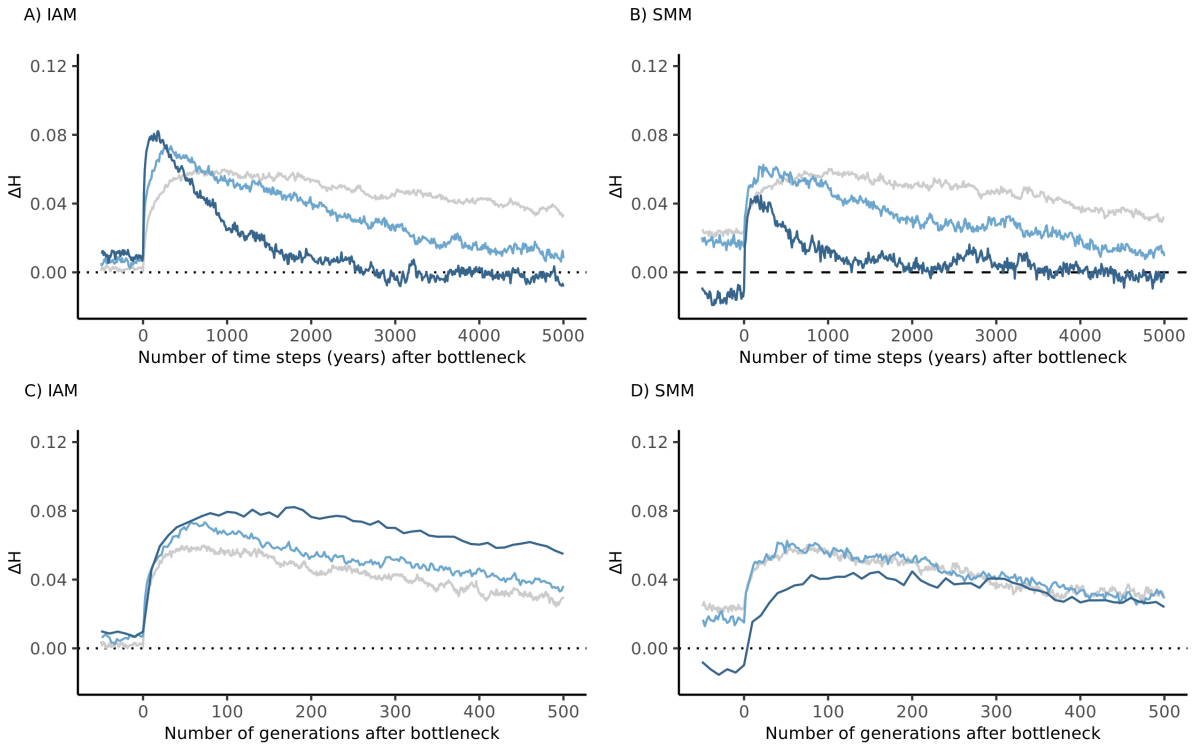

Figure S4. Temporal dynamics of Δ*H* calculated from stochastic simulations of microsatellite markers evolving under IAM (panels A and C) or SMM (panels B and D) in a single population that went from 1000 to 500 individuals within a single time step at time 0. Top and bottom figures show the same data with time expressed either in years (A and B) or generations (C and D). The dark blue curve corresponds to a population without overlapping generations (adult survival *v*=0, generation time T_G=1 year), while the light blue and grey curves correspond to adult survival *v*=0.8 (T_G=4.5 years) and *v*=0.95 (T_G=13.4 years).

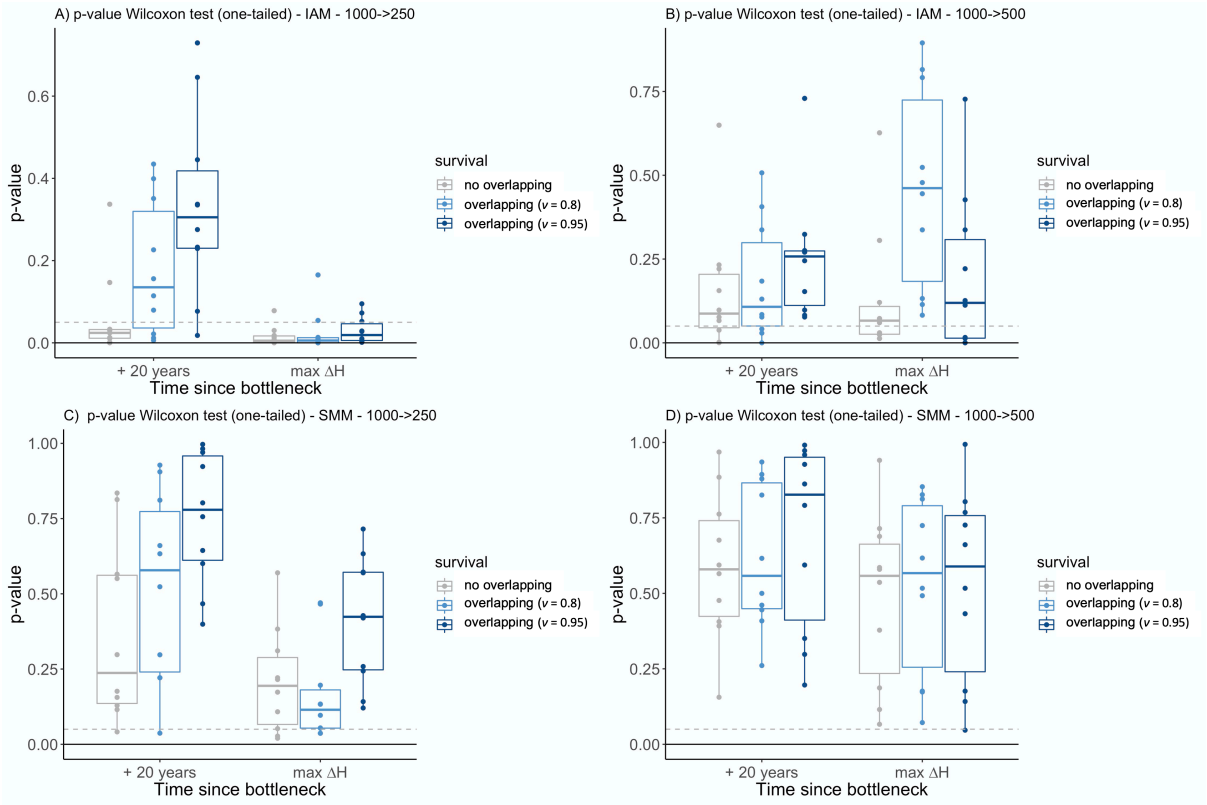

Figure S5. One-tailed p-values obtained when testing an excess of heterozygotes with a Wilcoxon test in *Bottleneck* based on genetic data obtained from stochastic simulations of microsatellite markers evolving under IAM (panels A and B) or SMM (panels C and D) in a single population that went from 1000 to 250 individuals (panels A and C) or from 1000 to 500 individuals (panels B and D) at the peak of ΔH and 20 years after the decline.

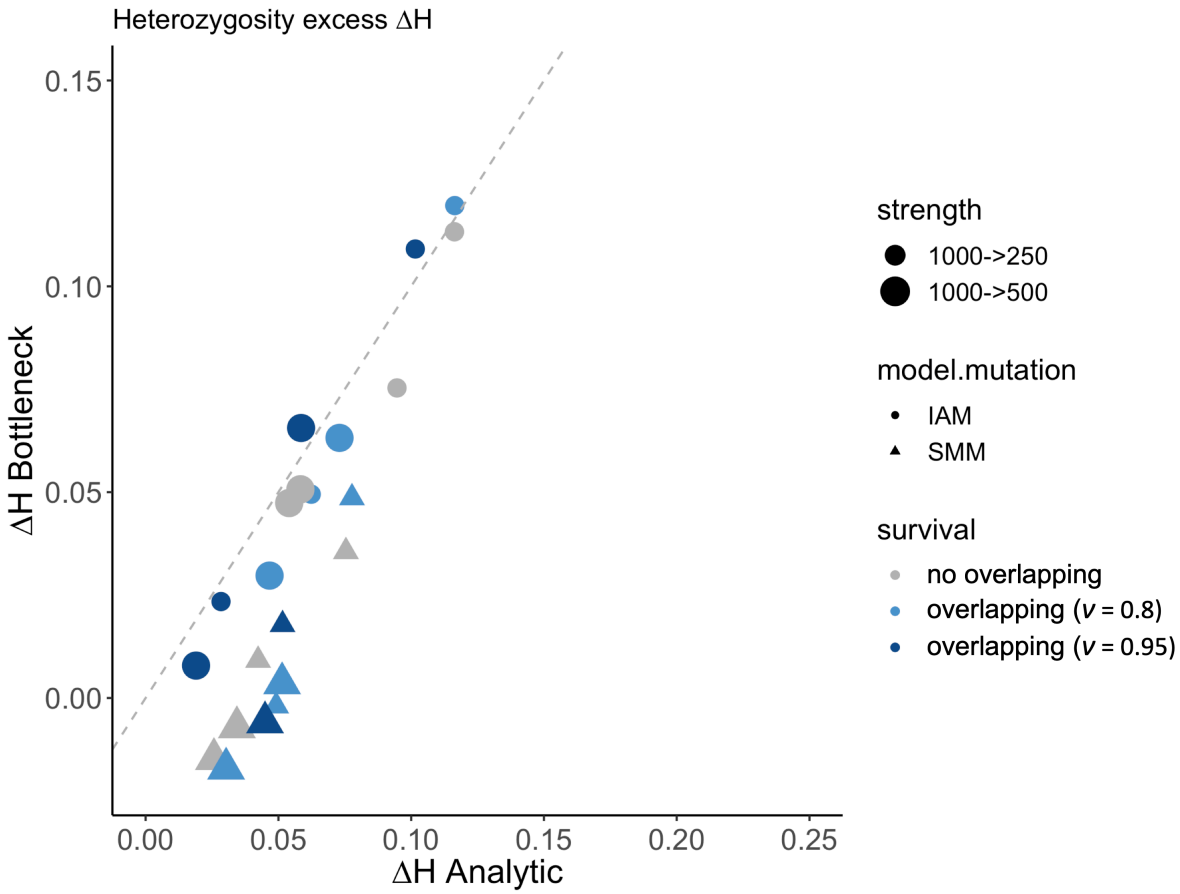

Figure S6. Comparison of our analytical estimates of Δ*H* (x-axis) against the Δ*H* values estimated by *Bottleneck* (y-axis), from genetic data obtained from stochastic simulations of microsatellite markers evolving under IAM or SMM in a single population that went from 1000 to 250 individuals or from 1000 to 500 individuals at the peak of ΔH and 20 years after the decline, under three survival models, where *v* correspond to adult survival *v*=0.8 and *v*=0.95 in overlapping generation models.

References

Andrews S (2010). FastQC: a quality control tool for high throughput sequence data. Available online at: http://www.bioinformatics.babraham.ac.uk/projects/fastqc.

Brelsford A, Dufresnes C, Perrin N (2016). High-density sex-specific linkage maps of a European tree frog (*Hyla arborea*) identify the sex chromosome without information on offspring sex. *Heredity* **116**: 177–181.

Catchen JM, Amores A, Hohenlohe P, Cresko W, Postlethwait JH (2011). *Stacks*: Building and genotyping loci *de novo* from short-read sequences. *G3: Genes|Genomes|Genetics* **1**: 171.

Catchen JM, Hohenlohe PA, Bassham S, Amores A, Cresko WA (2013). Stacks: an analysis tool set for population genomics. *Molecular Ecology* **22**: 3124–3140.

Cotto O, Schmid M, Guillaume F (2020). Nemo-age: spatially explicit simulations of eco-evolutionary dynamics in stage-structured populations under changing environments. *Methods in Ecology and Evolution* **11**: 1227–1236.

Ewels P, Magnusson M, Lundin S, Käller M (2016). MultiQC: summarize analysis results for multiple tools and samples in a single report. *Bioinformatics* **32**: 3047–3048.

Fraïsse C, Popovic I, Mazoyer C, Spataro B, Delmotte S, Romiguier J, *et al.* (2021). DILS: Demographic inferences with linked selection by using ABC. *Molecular Ecology Resources* **in press**.

Gaillard J -M., Yoccoz NG, Lebreton J -D., Bonenfant C, Devillard S, Loison A, *et al.* (2005). Generation Time: A Reliable Metric to Measure Life-History Variation among Mammalian Populations. *The American Naturalist* **166**: 119–123.

Knaus BJ, Grünwald NJ (2017). vcfR: a package to manipulate and visualize variant call format data in R. *Molecular Ecology Resources* **17**: 44–53.

Leblois R, Pudlo P, Néron J, Bertaux F, Reddy Beeravolu C, Vitalis R, *et al.* (2014). Maximum-Likelihood Inference of Population Size Contractions from Microsatellite Data. *Molecular Biology and Evolution* **31**: 2805–2823.

Mastretta-Yanes A, Arrigo N, Alvarez N, Jorgensen TH, Piñero D, Emerson BC (2015). Restriction site-associated DNA sequencing, genotyping error estimation and de novo assembly optimization for population genetic inference. *Molecular Ecology Resources* **15**: 28–41.

Nunney L (1993). The influence of mating system and overlapping generations on effective population size. *Evolution* **47**: 1329–1341.

Peterson BK, Weber JN, Kay EH, Fisher HS, Hoekstra HE (2012). Double digest RADseq: an inexpensive method for *de novo* SNP discovery and genotyping in model and non-model species. *Plos One* **7**.

R Development Core Team (2020). R: a language and environment for statistical computing. R Foundation for Statistical Computing, Vienna.